Chapter 16

Absorption Features

As expressed by Eq. 5.31, the measured counts in a spectrum exhibiting absorption are

$$I_\lambda = I_\lambda^0 \exp\{-\tau_\lambda\} = I_\lambda^0 \exp\{-N\sigma(\lambda)\}, \tag{16.1}$$

where τ_λ is the optical depth, N is the column density (Eq. 5.13), and $\sigma(\lambda)$ is the total absorption cross section (Eq. 5.29). The optical depth, and therefore Eq. 16.1, is formulated based upon statistical and probabilistic treatment of the absorption process.

In this chapter, we present the bound–bound and bound–free atomic absorption cross sections. The total absorption cross section for bound–bound absorption, known as the Voigt profile, is also presented. In addition, we introduce the well–known equivalent width and the curve of growth for bund–bound absorption profiles. The most commonly observed bound–free absorption is the ionization of ground–state neutral hydrogen, known as Lyman–limit absorption; we present the atomic cross section and absorption behavior for this bound–free transition.

16.1 Bound–bound absorption cross section

The bound–bound atomic absorption cross section, $\alpha(\lambda)$, has a highly peaked and very narrow functional form with wavelength. The wavelength of the peak, the amplitude of the peak, and the width of the cross section are dictated by the atomic constants governing the given bound–bound transition.

Per Eq. 4.34, the integral of the cross section provides fractional power absorbed from the beam per transition. For atomic bound–bound transitions, the

factional power absorbed is

$$\int_0^\infty \alpha(\lambda)\, d\lambda = \pi f \frac{e^2 \lambda_r^2}{m_e c^2}, \tag{16.2}$$

where λ_r is the wavelength at which $\alpha(\lambda)$ peaks (corresponding to the resonance frequency, $\nu_r = c/\lambda_r$), and f is the oscillator strength.

16.1.1 The Lorenztian

The functional form of atomic absorption cross sections for bound–bound transitions are known as Cauchy probability distribution functions, Breit–Wigner distribution functions, or more commonly by physicists and astronomers as Lorentz distribution functions (or simply "the Lorentzian").

In the most simple form, the Lorentzian is written

$$\mathcal{L}(x) = \frac{1}{\pi} \frac{y}{(x - x_0)^2 + y^2} = \frac{1}{\pi} \frac{y}{(\Delta x)^2 + y^2}, \tag{16.3}$$

where $\Delta x = x - x_0$. The peak of $\mathcal{L}(x)$ is at x_0, which is known as the location parameter. The amplitude at the peak is $1/\pi y$, thus, y is known as the scale parameter. The half–width at half–maximum, FWHM/2, is also equal to y.

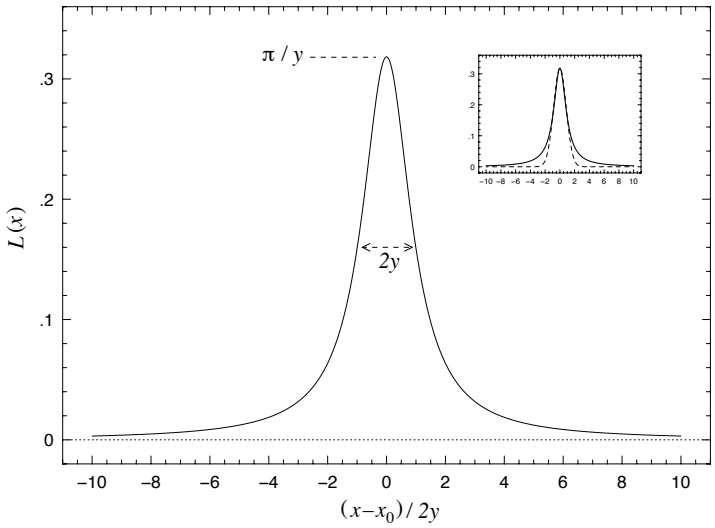

Figure 16.1: The Lorentzian distribution function given by Eq. 16.3 as a function of $(x - x_0)/2y$. The function has unity area, so that the amplitude at the peak is $1/\pi y$ when the full width half maximum is $2y$. (inset) The same Lorentzian (solid curve) with a Gaussian distribution (dashed curve) having the same FWHM and amplitude as the Lorentzian. Note that the wings of the Lorentzian are highly extended compared to the similar Gaussian distribution.

A Lorentzian centered at $\Delta x = 0$ is illustrated in Figure 16.1 as a function of $(x - x_0)/2y$. The essential characteristics of the Lorentzian is that the wings

of the distribution, defined in the regime $(x - x_0) \gg y$, decay very slowly, as $(x-x_0)^{-2}$, and are much more extended than those of a Gaussian function with the same FWHM and amplitude (see inset of Figure 16.1). The area under $\mathcal{L}(x)$ is unity,

$$\frac{1}{\pi}\int_0^\infty \frac{y}{(x-x_0)^2+y^2}\,dx = \frac{1}{\pi}\int_{-\infty}^\infty \frac{y}{(\Delta x)^2+y^2}\,d\Delta x = 1. \tag{16.4}$$

16.1.2 The cross section

Eq. 16.3 can then be written

$$\alpha(\lambda) = f\frac{e^2\lambda_r^2}{m_e c^2}\frac{\Gamma\lambda_r^2/4\pi c}{(\lambda-\lambda_r)^2+(\Gamma\lambda_r^2/4\pi c)^2}, \tag{16.5}$$

for which $y = \Gamma\lambda_r^2/4\pi c$. The FHWM is $\Delta\lambda = \Gamma_{mn}\lambda_{mn}^2/2\pi c$.

16.1.3 Atomic constants

The transition wavelength, the oscillator strength, and damping constan t constitute the atomic constants for each transition. In Table 16.1. the atomic constants are listed for selected transitions that are commonly seen in absorption in quasar spectra.

Table 16.1: Atomic Constants[a] for Selected Transitions

Ion/Tran	λ_{mn} [Å]	f_{mn}	Γ_{mn} [sec^{-1}]
Lyα	1215.670[b]	4.164×10^{-1}	6.265×10^{8}
Lyβ	1025.722[b]	7.912×10^{-2}	1.672×10^{8}
O VI λ1032	1031.9261[c]	1.329×10^{-1}	4.163×10^{8}
O VI λ1038	1037.6167[c]	6.609×10^{-1}	4.095×10^{8}
N V λ1238	1238.821	1.56×10^{-1}	3.40×10^{8}
N V λ1242	1242.804	7.80×10^{-2}	3.37×10^{8}
Si IV λ1393	1393.755	5.13×10^{-1}	8.80×10^{8}
Si IV λ1402	1402.770	2.55×10^{-1}	8.63×10^{8}
C IV λ1548	1548.187	1.90×10^{-1}	2.65×10^{8}
C IV λ1550	1550.772	9.52×10^{-2}	2.64×10^{8}
Mg II λ2796	2796.352	6.08×10^{-1}	2.60×10^{8}
Mg II λ2803	2803.531	3.03×10^{-1}	2.57×10^{8}

a Taken from the National Institute of Standards and Technology
b Quoted values weighted by branching ratio of both spin states
c Taken from Morton (1991)

Though oscillator strengths, f, and damping constants, Γ, can be expressed in terms of fundamental quantities, they are measured in the laboratory for each transition and carry an uncertainty of $\sim 10\%$.

Note that the amount of energy removed from the photon beam (in this case the quasar light) scales with $\lambda^2 f$ and has no dependence upon Γ. Thus, the relative magnitude of energy removed from the beam for the well–known doublets listed in Table 16.1 is proportional to the ratio of their $\lambda^2 f$ values. (Note, however that the wavelength difference for doublets is small).

For most doublets, the f values differ by a factor of two between the two transitions. In most all case the bluer transition in a doublet has a larger f value than that of the redder transition, i.e. $f_b = 2f_r$. However, there are rare cases where this is not the case, such as with the Si II $\lambda\lambda 1190, 1193$ doublet, for which $f_r = 2f_b$.

16.2 Voigt profile

The Voigt profile gives the distribution of absorption as a function of wavelength when the natural absorption coefficient per atom, $\alpha_{nat}(\lambda)$, is modulated by the Gaussian thermal distribution of atoms, $Nf(\Delta\lambda)$, where N is the column density. The optical depth, τ_λ, then, takes on the shape of the Voigt profile through the convolution

$$\tau_\lambda = N\alpha(\lambda) = N\alpha_{nat}(\lambda) \otimes f(\Delta\lambda), \tag{16.6}$$

An explicit writing of Eq. 16.6 is

$$\tau_\lambda = \int_{-\infty}^{\infty} N\alpha_{nat}(\lambda')f(\lambda' - \lambda)d\lambda', \tag{16.7}$$

which must be evaluated at each λ to obtain the observed line shape. Expanding gives

$$\tau_\lambda = N\frac{e^2\lambda_r^2}{m_e c^2} f \frac{\Gamma\lambda_r^2/4\pi c}{(\Delta\lambda)^2 + (\Gamma\lambda_r^2/4\pi c)^2} \otimes \frac{1}{\sqrt{\pi}\Delta\lambda_D} e^{-(\Delta\lambda/\Delta\lambda_D)^2}, \tag{16.8}$$

where the transition wavelength, λ_r, has been written explicitly, $\Delta\lambda = \lambda - \lambda_r$, and the oscillator stength, f, has been included into the normalization. Note the integral of $\alpha(\lambda)$ is still the energy per second per atom per square radian absorbed by the bound–bound transition, $(\pi e^2/mc)(\lambda^2/c)f$.

The convolution of a Lorentzian and a Gaussian is the Voigt function, u, which has unit normalization. The absorption coefficient with wavelength can be written

$$\tau_\lambda = N\frac{\pi e^2\lambda_r^2}{m_e c^2} f u(x,y) \quad \text{where} \quad u(x,y) = \frac{1}{\sqrt{\pi}\Delta\lambda_D} H(x,y) \tag{16.9}$$

and where the convolution is conveniently expressed by the Hjerting function,

$$H(x,y) = \frac{y}{\pi}\int_{-\infty}^{\infty} \frac{\exp(-t^2)}{(x-t)^2 + y^2} dt \tag{16.10}$$

with

$$x = \frac{\Delta\lambda}{\Delta\lambda_D} \quad \text{and} \quad y = \frac{\Gamma\lambda_r^2}{4\pi c}\frac{1}{\Delta\lambda_D}. \tag{16.11}$$

Note that x acts as the independent variable. It simply is the difference between the wavelength along the profile and the line center in units of the Doppler width. Also note that y is not a function of $\Delta\lambda$ and therefore does not vary with location across the absorption profile. For the given transition, y is a function of only the damping constant, the wavelength of the line center, and the Doppler width. As seen in Eq. 5.25, the latter depends upon the gas temperature, the wavelength of the line center, and the mass of the atom. Note that the Doppler width also appears in the normalization of the Voigt function, u, in Eq. 16.9.

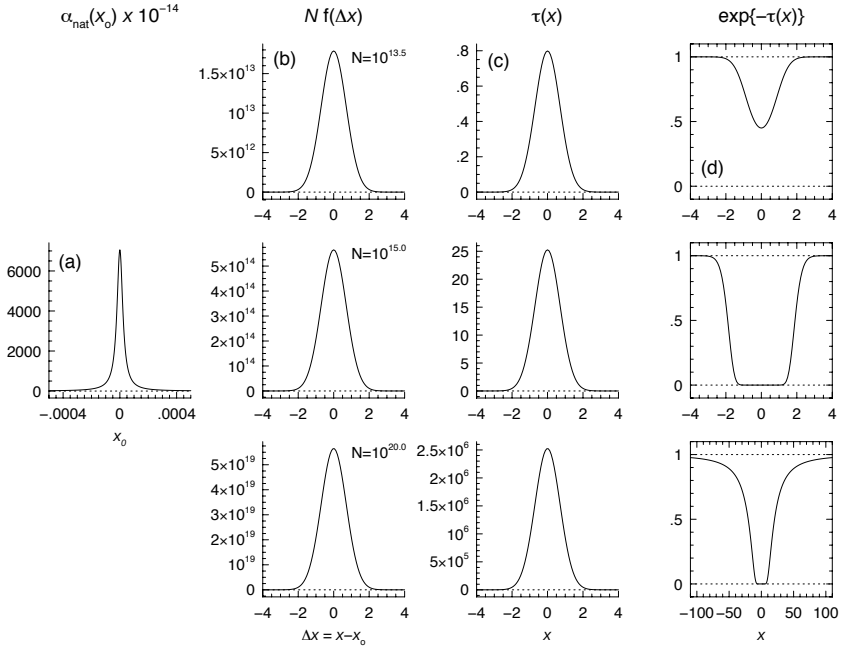

Figure 16.2: A schematic of the convolution process to obtain the observed line shape in units of $x = \Delta\lambda/\Delta\lambda_D$ for the Lyα transition. (*a*) The natural broadening per atom, $\alpha_{nat}(x_0)$. (*b*) The thermal distribution of atoms, $Nf(x - x_0)$ for $\log N = 13.5$, 15.0, and 20.0 [cm^{-2}] (from top to bottom). (*c*) the optical depth profile, $\tau(x)$, which is obtained via convolution of $\alpha_{nat}(x_0)$ and $Nf(x - x_0)$. (*d*) Application of Eq. 16.12 gives the absorption profile.

The observed absorption profile will then have the shape

$$I_\lambda = I_\lambda^o \exp\{-\tau_\lambda\}, \tag{16.12}$$

where I_λ is the observed flux at wavelength λ and I_λ^o is the quasar continuum flux (in the absence of the absorption line).

An illustration of the convolution process for obtaining Eq. 16.12 is shown in Figure 16.2 for Lyα transitions with $\log N = 13.5$, 15.0, and 20.0 [cm^{-2}] (from top to bottom). The Lorentzian (natural profile), $\alpha_{nat}(x_0)$, is shown in

Figure 16.2*a* for an atom centered at location x_0. Note the extreme narrowness of the profile, plotted over the range $-0.0005 \leq x_0 \leq 0.0005$; the width is governed by $\Gamma\lambda_r^2/4\pi c$. Convolution with Eq. 5.26 scaled by the total column density, $Nf(x - x_0)$, shown in Figure 16.2*b*, modulates for the thermal distribution of atoms at each x_o, and yields the optical depth, $\tau(x)$, as shown in Figure 16.2*c*. Note that, for the small x ranges shown (near the line centers) the $\tau(x)$ profile shapes emulate the shape of $f(\Delta x)$; i.e., they follow the shape of a Gaussian function. This is because the width of the Lorentzian is extremely narrow. However, the amplitudes vary by orders of magnitude depending upon N. For the $\log N = 13.5$ cm^{-2} case, $\tau(x) < 1$ for all x and the observed profile in Figure 16.2*d* (top panel) is not saturated. For the $\log N = 15.0$ cm^{-2} case, $\tau(x) > 1$ for $|x| < 2$, yielding a highly saturated observed profile in Figure 16.2*d* (center panel). As the column density is increased to $\log N = 20.0$ cm^{-2}, $\tau(x) > 1$ for $|x| < 20$, so that $\tau(x)$ is non–negligible at large x. In this case, the wings of $\tau(x)$ are governed by the extended wings of the Lorentzian, which become important contributors to the absorption profile shape. The extended wings of the profile, shown in Figure 16.2*d* (lower panel) are called damping wings. This is in reference to damping constant, Γ, appearing in the Lorentzian.

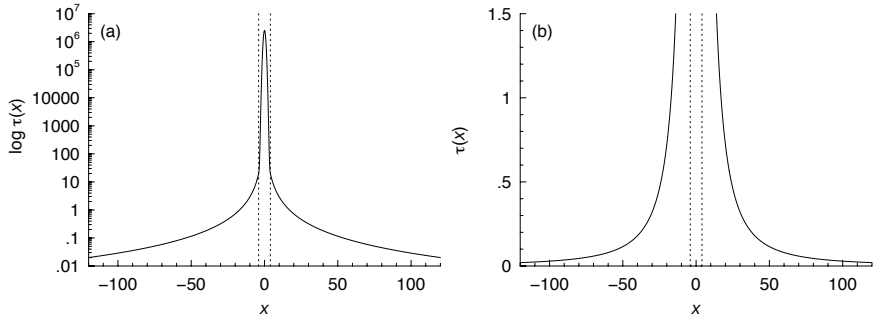

Figure 16.3: (*a*) The logarithmic optical depth, $\log \tau(x)$, reproduced from Figure 16.2*d* for the $\log N = 20.0$ cm^{-2} case over the range $-120 \leq x \leq 120$. Note that the optical depth is non–negligible for large x. (*b*) The same optical depth profile, in an expanded view. Note how the wings of the optical depth emulate those of Lorentzian, $\alpha(x_0)$, giving rise to the so–called damping wings in the observed absorption profile (bottom panel of Figure 16.2*d*). Vertical dashed lines mark the x range shown in Figure 16.2.

An expanded scale of the $\log \tau(x)$ for $\log N = 20.0$ cm^{-2} is shown in Figure 16.3*a*. In Figure 16.3*b*, $\tau(x)$ is plotted versus x for $\tau(x) \leq 1.5$. Note that the optical depth remains non–negligible over the range $x \pm 100$, decreasing slowly per the wings of the Lorentzian for increasing x. These extended wings are what gives rise to the damping wings of the observed profiles, as shown in Figure 16.2*d* (lower panel). Thus, we see that the shape of the optical depth, Voigt profile behaves as a Gaussian function for small x (near the line core), and behaves as the wings of the Lorentzian, $\tau(x) \propto x^{-2}$, for large x. However, it is only in cases of large N that $\tau(x)$ is non–negligible beyond the line core.

Profiles such as those shown Figure 16.2*d* can be fit to Eq. 16.12 to objectively obtain the column density, N, and the only additional free parameter, the

Doppler width, $\Delta\lambda_D$. This approach is useful only for high resolution data in which the line width induced by the instrument (see § 6.10) is significantly less than the Doppler width. Usually the fitting of the data is performed using the technique of χ^2 minimization (§ 3.5). In high resolution spectra, the absorption lines often break up into multiple components, forming a complex and often blended profile shape. We will address this further complexity in Chapter 17.

16.3 Equivalent widths: curve of growth

The general definition of the equivalent width is

$$W = \int_{-\infty}^{\infty} \left(1 - \frac{I_\lambda}{I_\lambda^0}\right) d\lambda. \tag{16.13}$$

The units of W are wavelength units, such as Å. The equivalent width represents the width in wavelength of an absorption feature with $I_\lambda = 0$ across the profile (an inverted top hat function) with the identical amount of flux removed from the photon beam. It is also a conserved quantity in that it is independent of the line shape and the resolution of the spectrograph (see below).

Recall that the shape of an absorption profile is given by

$$I_\lambda = I_\lambda^0 \exp\{-\tau_\lambda\} = I_\lambda^0 \exp\{-N\alpha(\lambda)\}. \tag{16.14}$$

Rewriting Eq. 16.13 by substituting Eq. 16.14, we have

$$W = \int_{-\infty}^{\infty} [1 - \exp\{-\tau_\lambda\}]\, d\lambda. \tag{16.15}$$

A schematic illustrating the interpretation of the equivalent width is shown in Figure 16.4 for $W = 0.21$ Å. The integral of the flux remove from the incident light beam is identical for each of the very different absorption profiles. The shaded grey area is the "equivalent profile" with zero flux. The width of this "equivalent profile" is the equivalent width.

As can be seen in Figure 16.4, there can be a family of $N\alpha(\lambda)$ combinations for fixed W. That is, the equivalent width is degenerate for various combinations of column density, N, and absorption coefficient, $\alpha(\lambda)$. For a given atomic transition, the shape of $\alpha(\lambda)$ is governed by $\Delta\lambda_D$ of the Gaussian component to the Voigt function (see Eq. 16.9). Recall that $\Delta\lambda_D$ is proportional to the Doppler b parameter, which is used to characterize the thermal and/or turbulent component to the line broadening.

As shown above, the equivalent width is related to N and b through the optical depth, $\tau_\lambda = N\alpha(\lambda)$. The behavior of the equivalent width dependence on N and b is called the curve of growth, or COG. As the optical depth of the line increases, the equivalent width also increases, however the precise functional dependence is sensitive to the optical depth at the line core, τ_o.

As τ_o increases, the line depth increases until all the photons at the line core are removed from the incoming beam. At this point, the absorption line

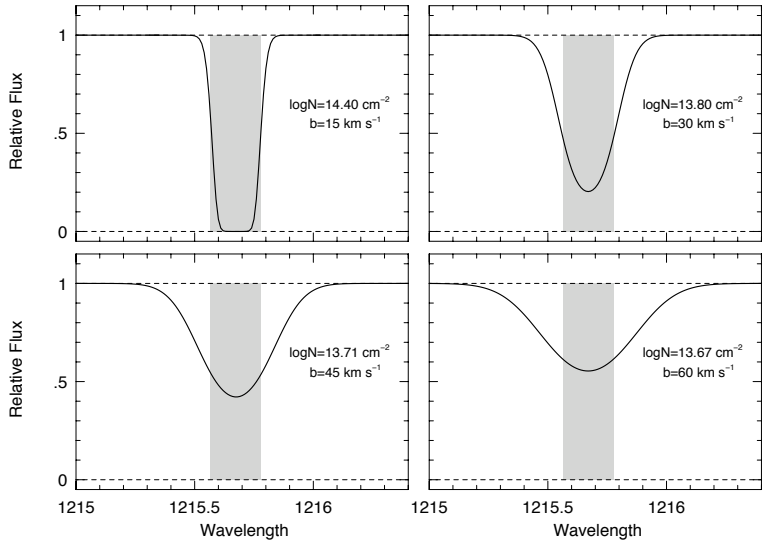

Figure 16.4: A schematic of four absorptions lines each with equivalent width $W = 0.21$ Å. Though the line profile shapes are quite different, the total amount of flux absorbed, as given by Eq. 16.15, are identical. The shaded grey area shows the interpretation of the equivalent width.

is considered to be "saturated". As τ_o increases further, very little additional light is removed from the beam until a regime in which damping wings form at very large τ_o. At these large τ_o values, the majority of the light is removed far from line center. These three regimes of behavior are called the "linear", "flat", and "damped" parts of the COG respectively. These are often refereed to as the linear, logarithmic, and square root regimes of the curve of growth due to the functional dependence upon the column density, N. Note that only in the logarithmic part will W be sensitive to the b parameter, and thus the Gaussian component of the line broadening.

In the following sections, the functional dependence of the COG will be examined in detail. For regime of behavior along the COG, a dominant physical process is at play, and this will guide the derivation of τ_o for each of the three parts of the COG. In short, we have

$$\begin{aligned} W \propto N \qquad & \tau_o \ll 1 \qquad & \tau_o = \frac{\pi e^2}{mc^2}\lambda^2 N f \\ W \propto b\sqrt{\ln(N/b)} \quad & 10 \leq \tau_o \leq 10^3 \quad & \tau_o = \frac{\pi^{1/2} e^2}{mc}\frac{\lambda}{b} N f \\ W \propto \sqrt{N} \qquad & \tau_o \geq 10^4 \qquad & \tau_o = \frac{1}{4}\frac{e^2 \Gamma}{mc^3}\lambda^4 N f \end{aligned} \tag{16.16}$$

In Figure 16.5, the COG for the Lyα ($n = 1 \rightarrow 2$) transition of HI is

shown for $b = 30$ km sec^{-1} as a function of τ_o. The thick portions of the curves correspond to the flat, logarithmic, and square root parts of the COG, based upon the slope of the curve on a log–log diagram. Insets show the Lyα absorption profiles for locations on the COG, marked with filled circles, in each regime with increasing τ_o.

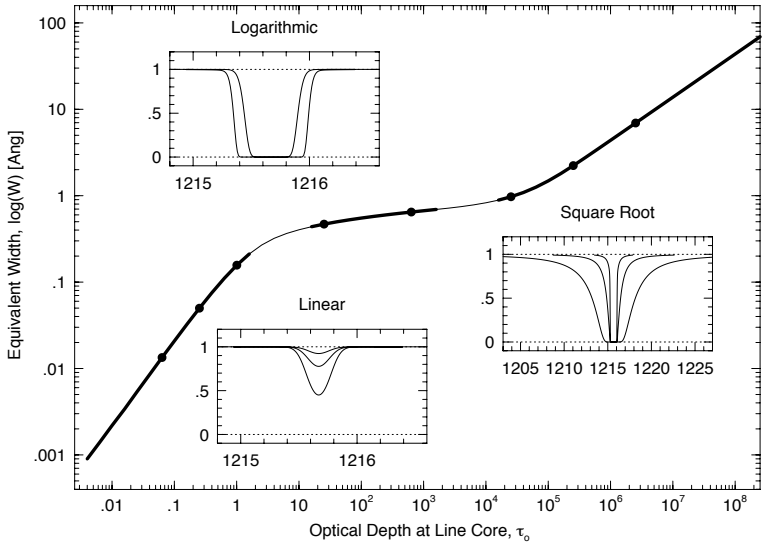

Figure 16.5: The COG showing equivalent width as a function of the optical depth at line core, τ_o, for Lyα for $b = 30$ km sec^{-1}. The three regimes, "linear", "logarithmic", and "square root", corresponding to Eq. 16.17, are shown by the thick curves, respectively, as τ_o increases. Absorption profiles are shown for each regime and their locations on the COG marked with filled points. Note the expanded wavelength scale for the profiles on the square root part of the COG. This is due to large damping wings.

16.3.1 The linear regime

In the optically thin regime, the optical depth in the line core is small, $\tau_o \ll 1$. Using series expansion of the exponential, we can approximate $\exp(-\tau_\lambda) \simeq -\tau_\lambda$. Substituting into Eq. 16.15, gives

$$W = \int_{-\infty}^{\infty} \tau_\lambda d\lambda = N \int_{-\infty}^{\infty} \alpha(\lambda) d\lambda \tag{16.17}$$

Substituting Eq. 16.9 for $\alpha(\lambda)$, we have

$$W = \frac{\pi e^2}{mc} \frac{\lambda^2}{c} N f \int_{-\infty}^{\infty} u(x,y) d\lambda = \tau_o \int_{-\infty}^{\infty} u(x,y) d\lambda, \tag{16.18}$$

which defines τ_o, where $u(x,y)$ is the Voigt function given by Eq. 16.11. By definition the Voigt function has unity normalization, so the integral in Eq. 16.18

equals unity and we have the linear functional dependence, $W \propto N$,

$$W = \frac{\pi e^2}{mc}\frac{\lambda^2}{c}Nf. \tag{16.19}$$

Note that the shape of $u(x, y)$ depends upon the Doppler width, $\Delta\lambda_D \propto b$, and is thus dependent upon the gas temperature. However, W is an integrated quantity and, because the Voigt function has unity normalization, is independent of b in the regime of $\tau_o \ll 1$.

Physically, in the regime of small τ_o, as more atoms are added to the absorbing gas, W grows by a deepening of the line core due to the removal of additional photons in the beam.

16.3.2 The logarithmic regime

In the regime where $10 \leq \tau_o \leq 10^3$, the damping wings of the Lorentzian are insignificant compared to those of the Gaussian contribution, and we can treat the Lorentzian contribution to the absorption coefficient as a δ function. We can write the optical depth as

$$\tau_\lambda = N\alpha(\lambda) \simeq \frac{\pi e^2\lambda^2}{mc^2}Nf\frac{1}{\pi^{1/2}\Delta\lambda_D}\exp\left[-\left(\frac{\Delta\lambda}{\Delta\lambda_D}\right)^2\right]. \tag{16.20}$$

Defining $\tau_o = (\pi e^2\lambda^2/mc^2)(1/\pi^{1/2}\Delta\lambda_D)Nf$, the optical depth of the line core, and invoking $x = (\Delta\lambda/\Delta\lambda_D)$, we can simplify the above equation to

$$\tau_\lambda = \tau_o \exp(-x^2). \tag{16.21}$$

From Eq. 16.15, the equivalent width is then

$$W = \Delta\lambda_D \int_{-\infty}^{\infty}\left[1 - \exp(-\tau_o e^{-x^2})\right]dx = \Delta\lambda_D F(\tau_o) \tag{16.22}$$

where

$$F(\tau_o) = \int_{-\infty}^{\infty}\left[1 - \exp(-\tau_o e^{-x^2})\right]dx \tag{16.23}$$

$$= \frac{\pi^{1/2}}{2}\sum_{n=1}^{\infty}\frac{(-1)^{n-1}\tau_o^n}{n!n^{1/2}}. \tag{16.24}$$

In the "flat" part of the curve of growth, the line core is saturated, meaning that W does not grow due to removal of photons with small x, where the Lorentzian dominates. The function $F(\tau_o)$ provides the behavior of the line absorption strength in the regime where the width of the line is governed by a Gaussian broadening mechanism. As τ_o is increased, the amplitude of the Gaussian increases and the wings of the line remove more flux from the beam. Physically, as more atoms are added to the gas, it is those in the tails of the

Doppler velocity distribution that contribute to increasing W. Thus, as we shall see below, $W \propto b$ for a fixed N.

For small τ_o, a series expansion of Eq. 16.21 yields Eq. 16.19 for the linear part of the curve of growth. When τ_o is large, series expansion yields the asymptotic solution

$$F(\tau_o) = (\ln \tau_o)^{1/2}\,, \tag{16.25}$$

which gives

$$W = \Delta\lambda_D\,(\ln \tau_o)^{1/2}\,. \tag{16.26}$$

From Eq. **??**, $b = (c/\lambda)\Delta\lambda_D$, and we have the full form of W written as

$$W = b\frac{\lambda}{c}\left(\ln\left[\frac{\pi^{1/2}e^2}{mc}\frac{\lambda}{b}Nf\right]\right)^{1/2}\,. \tag{16.27}$$

16.3.3 The square root regime

In this regime, where $\tau_o > 10^4$, the Lorentzian dominates due to very strong and broad wings. In this case, the Gaussian contribution to the Voigt function can treated as if it were a δ function. Thus, we can write the optical depth as

$$\tau_\lambda = N\alpha(\lambda) \simeq \frac{\pi e^2\lambda^2}{mc^2}Nf\frac{\Gamma\lambda^2/4\pi c}{(\Delta\lambda)^2 + (\Gamma\lambda^2/4\pi c)^2} \tag{16.28}$$

where $\alpha(\lambda)$ is given by Eq. 16.5. Defining $\beta = \Gamma\lambda^2/4\pi c^2$, we rewrite this as

$$\tau_\lambda = \frac{\pi e^2\lambda^2}{mc^2}Nf\frac{\beta}{(\Delta\lambda)^2 + \beta^2} \tag{16.29}$$

Due to the behavior of the Lorentzian, the majority of the energy removed from the beam is in wings of the absorption line. Thus, the equivalent width is dominated by regions under the line profile that are far from the line center. Under this assumption, $\Delta\lambda \gg \beta$, which leads to the approximation

$$\tau_\lambda = \frac{\pi e^2\lambda^2}{mc^2}Nf\frac{\beta}{(\Delta\lambda)^2}\frac{1}{1 + (\beta/\Delta\lambda)^2} \simeq \frac{\tau_o}{(\Delta\lambda)^2}, \tag{16.30}$$

where we define $\tau_o = \beta(\pi e^2\lambda^2/(mc^2)Nf$, the optical depth at the line center. Substituting this into Eq. 16.13, we have

$$W \simeq \int_{-\infty}^{\infty}\left[1 - \exp(-\tau_o/(\Delta\lambda)^2)\right]d\lambda. \tag{16.31}$$

The functional dependence of W can be obtained by a change of variable. Let $u^2 = (\Delta\lambda)^2/\tau_o$, then $du = d\lambda/\sqrt{\tau_o}$. Substituting onto the above integral, we have

$$W \simeq \tau_o^{1/2}\int_{-\infty}^{\infty}\left[1 - \exp(-1/u^2)\right]du = \tau_o^{1/2}F \tag{16.32}$$

where F is the value of the integral (a Gamma function, but yields a constant because there is no dependence upon τ_o). Writing out τ_o fully, we have

$$W \simeq F\frac{\lambda^2}{c^2}\left(\frac{e^2}{4m}\Gamma N f\right)^{1/2}. \tag{16.33}$$

Note that $W \propto \sqrt{\Gamma N}$, giving this regime either the name "square root" or "damping" part of the curve of growth.

16.3.4 Doublet ratios

In Figure 16.6, the COGs are shown for the often observed transitions Lyα λ1215, MgII λ2796, CIV λ1548, and OVI λ1031. The point of the illustration is that each of the COGs have very similar behavior. The only distinctions are the column density regimes of the three main parts of the COGs. In practice, only the Lyα transition is observed on the square root (damping) part of the COG.

However, it can be challenging to deduce the column density in the logarithmic (flat) part of the COG. In this regime, it is necessary to include information from additional transition from the same ionic species.

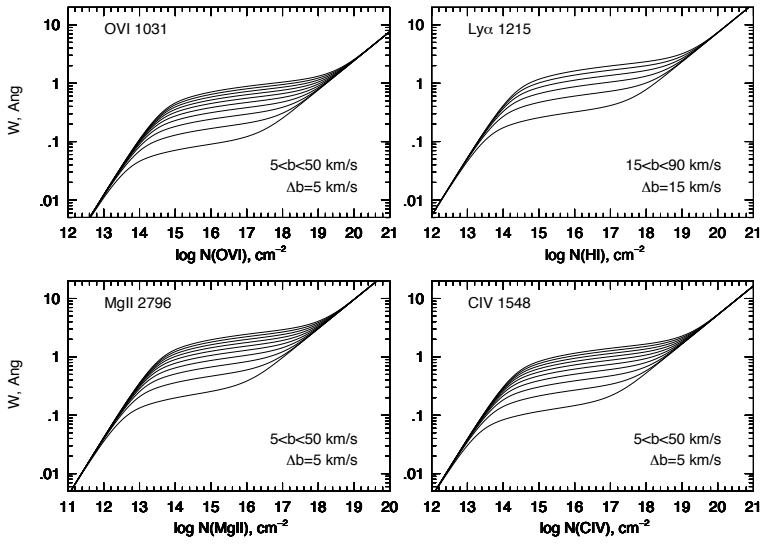

Figure 16.6: The curve of growth for Lyα λ1215, MgII λ2796, CIV λ1548, and OVI λ1031. For each species, the equivalent width, W, [Å] is plotted vs. the logarithm of the column density. For the curves shown, the range of b parameters are given in the lower right corner of the panels, with b increasing in steps of Δb upward.